Electronic Supplementary Information (ESI)

on

Triplet-triplet annihilation photon upconversion from diphenylhexatriene and its ring-substituted derivatives solution

Toshiko Mizokuro,[1*] Kenji Kamada[2] and Yoriko Sonoda[1]

[1]*RIAEP, National Institute of Advanced Industrial Science and Technology (AIST), 1-1-1 Higashi, Tsukuba, Ibaraki 305-8565, Japan.*
[2]*NMRI, National Institute of Advanced Industrial Science and Technology (AIST), 1-8-31 Midorigaoka, Ikeda, Osaka 563-8577, Japan.*

**E-mail: mizokuro-t@aist.go.jp*

CONTENTS

1. Synthesis of pico DPH and jul DPH

General

HR-MS data were obtained using a Hitachi M80B spectrometer. ^{1}H and ^{13}C NMR spectra were recorded on a Bruker Avance 400 spectrometer (400 MHz and 100 MHz, respectively) with tetramethylsilane (TMS) as internal reference. The spectra are displayed in Figures S1 and S2.

(*E,E,E*)-1,6-Bis[4-(di-2-picolylamino)phenyl]hexa-1,3,5-triene (**pico DPH**)

To a solid mixture of 4-(di-2-picolylamino)benzaldehyde [1] (1.52 g, 5.0 mmol) and (*E*)-2-butene-1,4-bis(tributylphosphonium chloride) (0.66 g, 1.25 mmol) was added a solution of sodium ethoxide in ethanol (0.83 M, 3 mL) at 45 ºC under nitrogen atmosphere. After stirring for 2 h, ethanol (9 mL) was added to the reaction mixture. The resulting orange precipitate was filtered off, washed with water (60 mL), and dried. Recrystallization from ethanol. Yield 23 %. Mp 195 ºC. HR-MS calcd for $C_{42}H_{38}N_6$: 626.3158, found 626.3147; ^{1}H NMR ($CDCl_3$): δ = 8.58-8.60 (m, 4H; ring), 7.62 (td, J = 7.7, 1.8 Hz, 4H; ring), 7.16-7.25 (m, 12H; ring), 6.61-6.67 (m, 6H; ring and triene), 6.41 (d, J = 15.2, 2H; triene), 6.36 (dd, J = 6.9, 3.1 Hz, 2H; triene), 4.83 (s, 8H, methylene); ^{13}C NMR ($CDCl_3$): δ = 158.6, 149.8, 147.5, 136.9, 132.3, 131.5, 127.5, 127.1, 126.0, 122.1, 120.8, 112.7, 57.3.

(*E,E,E*)-1,6-Bis(5-julolidino)hexa-1,3,5-triene (**jul DPH**)

To a solid mixture of 9-julolidinecarboxaldehyde (TCI) (1.01 g, 5.0 mmol) and (*E*)-2-butene-1,4-bis(tributylphosphonium chloride) (0.66 g, 1.25 mmol) was added a solution of sodium ethoxide in ethanol (0.5 M, 5 mL) at 45 ºC under nitrogen atmosphere. After stirring for 2 h, ethanol (9 mL) was added to the reaction mixture. The resulting orange precipitate was filtered off, washed with ethanol (5 mL) and water (40 mL), and dried. Recrystallization from acetone. Yield 35 %. Mp 206 ºC (decomp). HR-MS calcd for $C_{30}H_{34}N_2$: 422.2722, found 422.2714; ^{1}H NMR ($CDCl_3$): δ = 6.85 (s, 4H; ring), 6.63 (ddd, J = 15.4, 6.9, 3.1 Hz, 2H; triene), 6.354 (d, J = 15.4 Hz, 2H; triene), 6.353 (dd, J = 7.0, 2.9 Hz, 2H; triene), 3.14 (t, J = 5.7 Hz, 8H; methylene), 2.74 (t, J = 6.5 Hz, 8H; methylene), 1.93-1.99 (m, 8H; methylene); ^{13}C NMR ($CDCl_3$): δ = 142.4, 131.9, 131.8, 125.4, 125.2, 125.0, 121.4, 50.0, 27.7, 22.1.

2. Quantum chemical calculation

Geometries of all DPH derivatives were optimzed at the B3LYP/6-31G(d) level of theory. The geometry optimizations were separately done for singlet ground state (S_0) and the lowest triplet state (T_1). The energy level of T_1 from S_0 was calculated as the difference in the total energy of the calculations. The energy levels of the lowest singlet excited state (S_1) from S_0, i.e., the transition energies, were calculated at the TD-CAM-B3LYP/6-31+G(d) level of theory by using the optimized geometries mentioned above. The use of the Coulomb-attenuating method (CAM) [2] improved the underestimation of the transition energies. The diffuse orbital was augmented to the basis set in the CAM-B3LYP calculation. The obtained results of S_1 transition energy reproduced the experimental result with good accuracy (0.14 eV or less, mostly within 0.05 eV). All calculations were performed by considering the solvent effect with self-consistent reaction filed (SCRF) method with the polarizable continuum model (PCM) for tetrahydrofuran (THF) on the program package Gaussian 16 [3].

3. Estimation of upconversion quantum efficiency at strong excitation limit (η_{UC}^{∞})

Upconversion quantum efficiency of TTA-UC is a function of excitation intensity I_{ex} as [4]

$$\eta_{UC}(I_{ex}) = \eta_{UC}^{\infty}\,\Theta(\Lambda), \tag{S1}$$

where

$$\Theta(\Lambda) = 1 + \frac{1 - \sqrt{1 + 2\Lambda(I_{ex})}}{\Lambda(I_{ex})} \tag{S2}$$

is *normalized upconversion quantum yield* and

$$\Lambda(I_{ex}) = \frac{2I_{ex}}{I_{th}} \tag{S3}$$

is *dimensionless excitation intensity*. I_{th} is threshold excitation intensity. $\Theta(\Lambda)$ approaches to unity when I_{ex} and $\Lambda(I_{ex})$ go infinity and η_{UC}^{∞} is *the quantum efficiency at the strong excitation limit*, where 100% of emitter triplets deactivate through the second-order reaction path of the concentration. Thus, this value represents the performance of system free from the influence of the emitter triplet concentration. Saturated quantum efficiency accessed by the experiments is just an approximate value of η_{UC}^{∞}.

If I_{th} is known, the value of $\eta_{\mathrm{UC}}^{\infty}$ can be deduced from I_{ex} and $\eta_{\mathrm{UC}}(I_{\mathrm{ex}})$, by putting I_{ex} and I_{th} into eq. S3, by putting the obtained $\Lambda(I_{\mathrm{ex}})$ into eq. S2, and by putting the obtained $\Theta(\Lambda)$ and $\eta_{\mathrm{UC}}(I_{\mathrm{ex}})$ into eq. S1. The deduced $\Lambda(I_{\mathrm{ex}})$, $\Theta(\Lambda)$, and $\eta_{\mathrm{UC}}^{\infty}$ from the I_{th} obtained by the excitation dependence of the UC emission intensity (Fig. S4) are shown in Table S1. The Linear curves with slopes1 and 2 that cross the calculated I_{th} are also shown in Figs. S4(f) and (g).

Table S1. I_{th}, Λ, Θ and $\eta_{\mathrm{UC}}^{\infty}$ values of the DPH derivatives obtained at excitation intensity of I_{ex} = 1.9 W cm^{-2}.

Compounds	I_{th} / W cm^{-2}	$\Lambda(I_{\mathrm{ex}})$	$\Theta(\Lambda)$	$\eta_{\mathrm{UC}}^{\infty}$
unsub.	3.1 ± 0.5	1.2 ± 0.2	0.30 ± 0.03	0.00086 ± 0.0001
NMe_2	3.0 ± 0.2	1.3 ± 0.09	0.31 ± 0.01	0.021 ± 0.003
CN	4.9 ± 0.4	0.78 ± 0.06	0.23 ± 0.01	0.003 ± 0.0003
pico	1.6 ± 0.3	2.4 ± 0.5	0.42 ± 0.04	0.036 ± 0.0035
jul	1.0 ± 0.1	3.8 ± 0.5	0.49 ± 0.02	0.024 ± 0.002

(a)

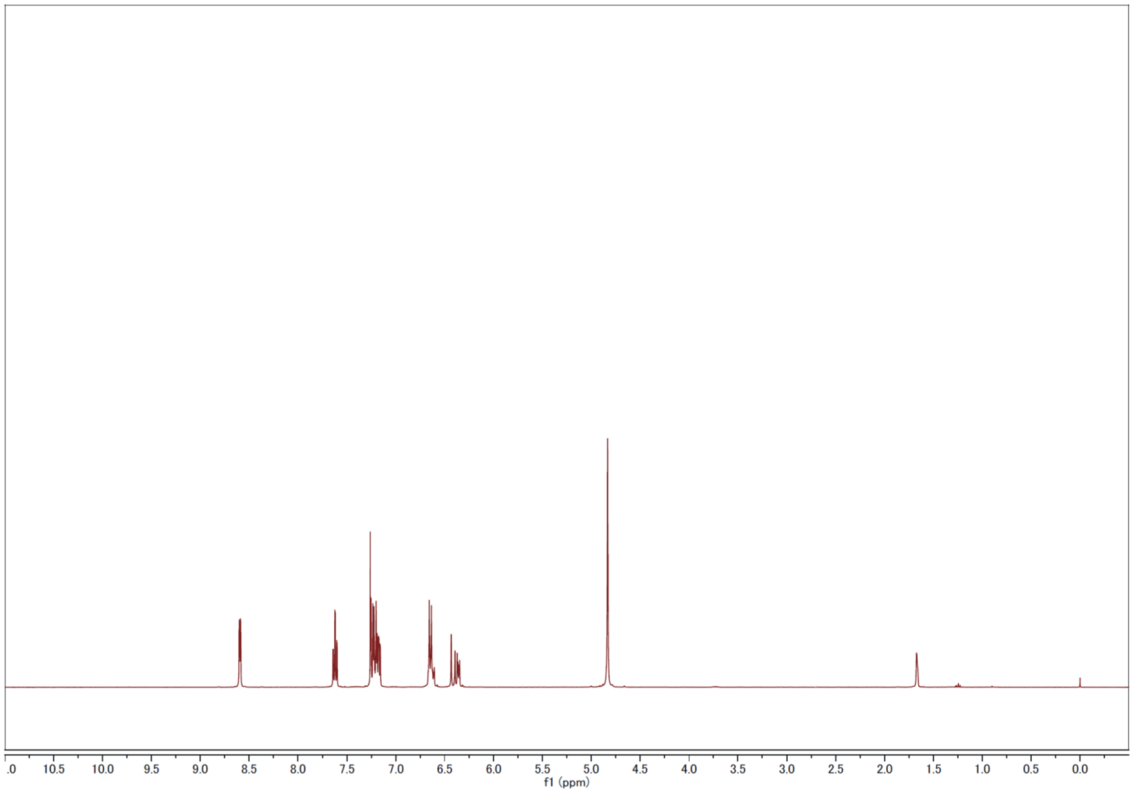

(b)

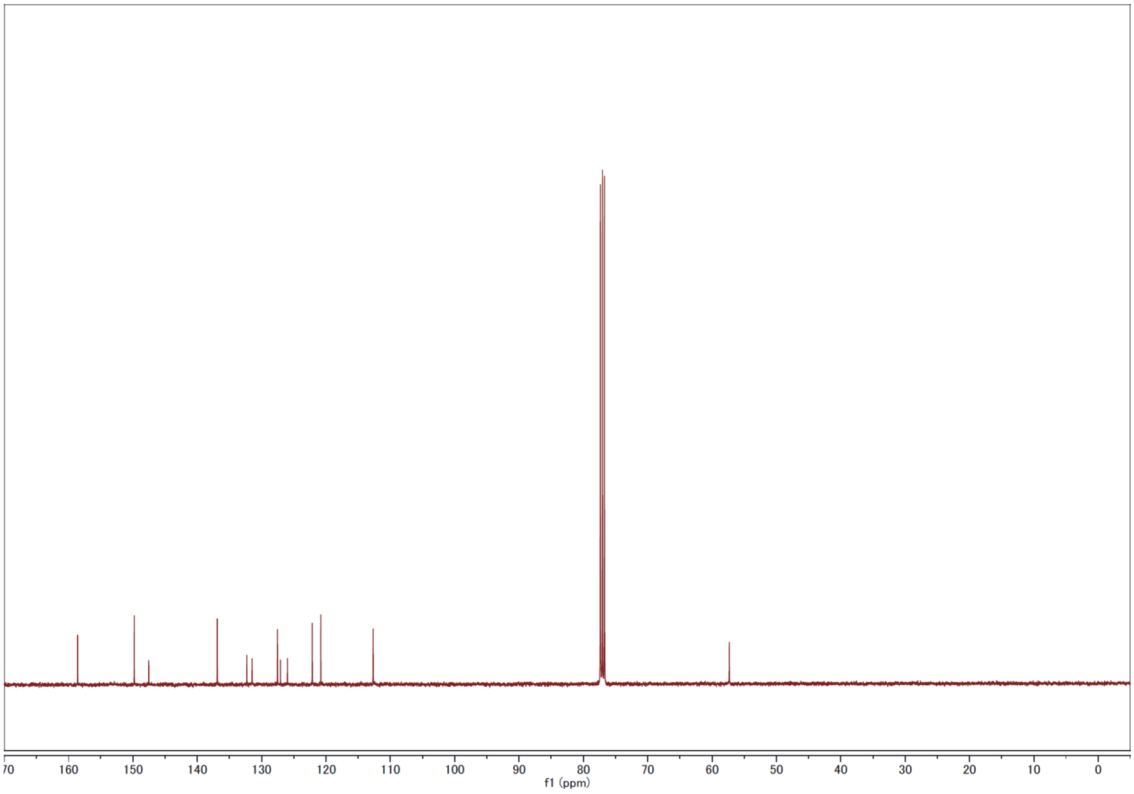

Figure S1. (a) ^{1}H and (b) ^{13}C NMR spectra of **pico DPH** in $CDCl_3$.

(a)

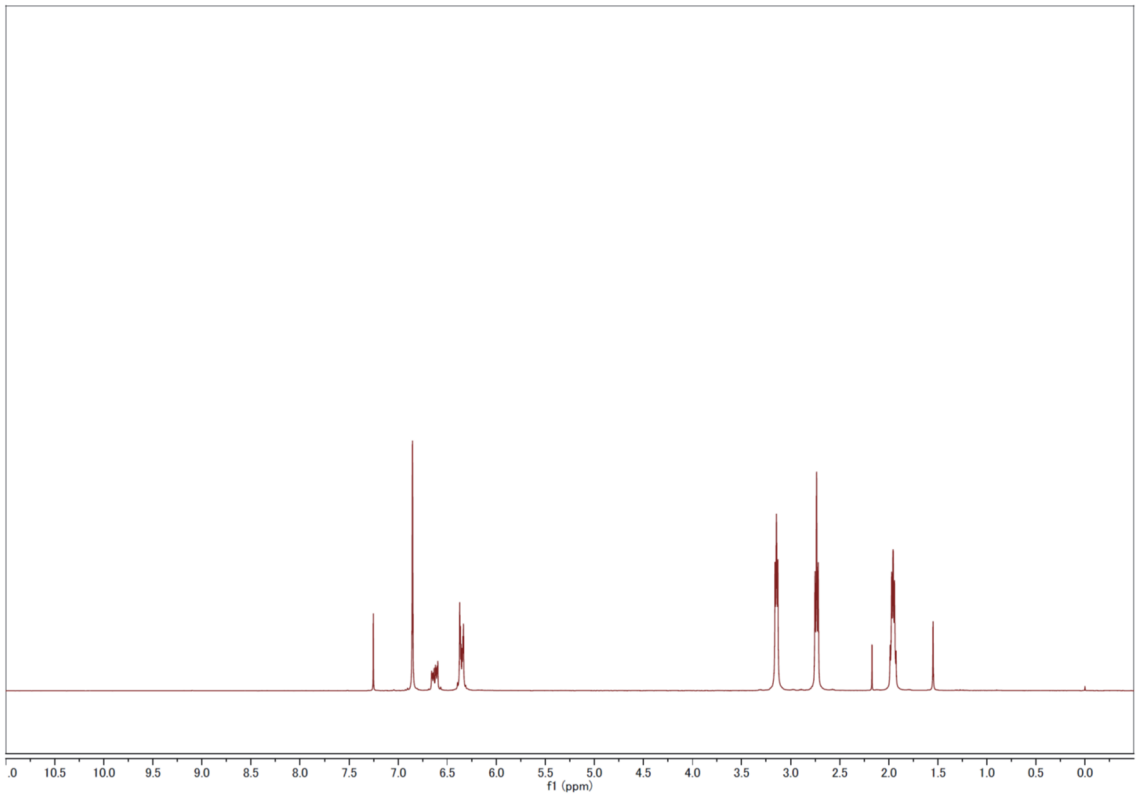

(b)

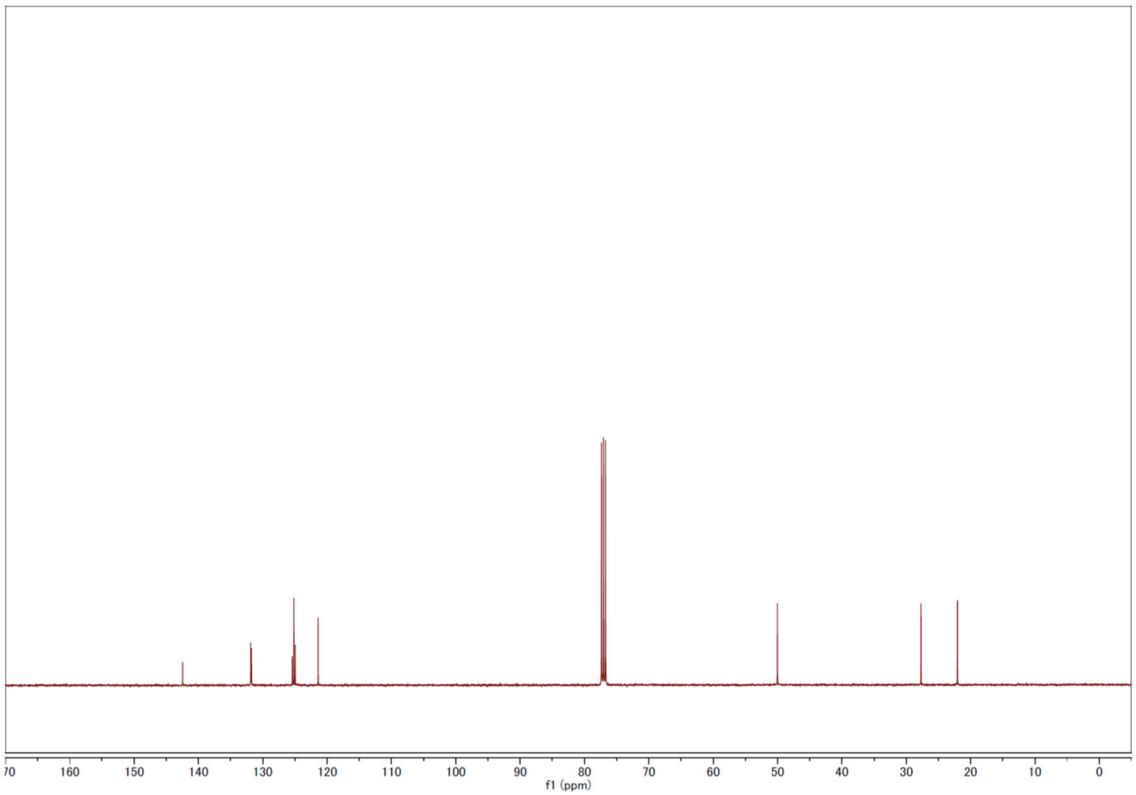

Figure S2. (a) ^{1}H and (b) ^{13}C NMR spectra of **jul DPH** in $CDCl_3$.

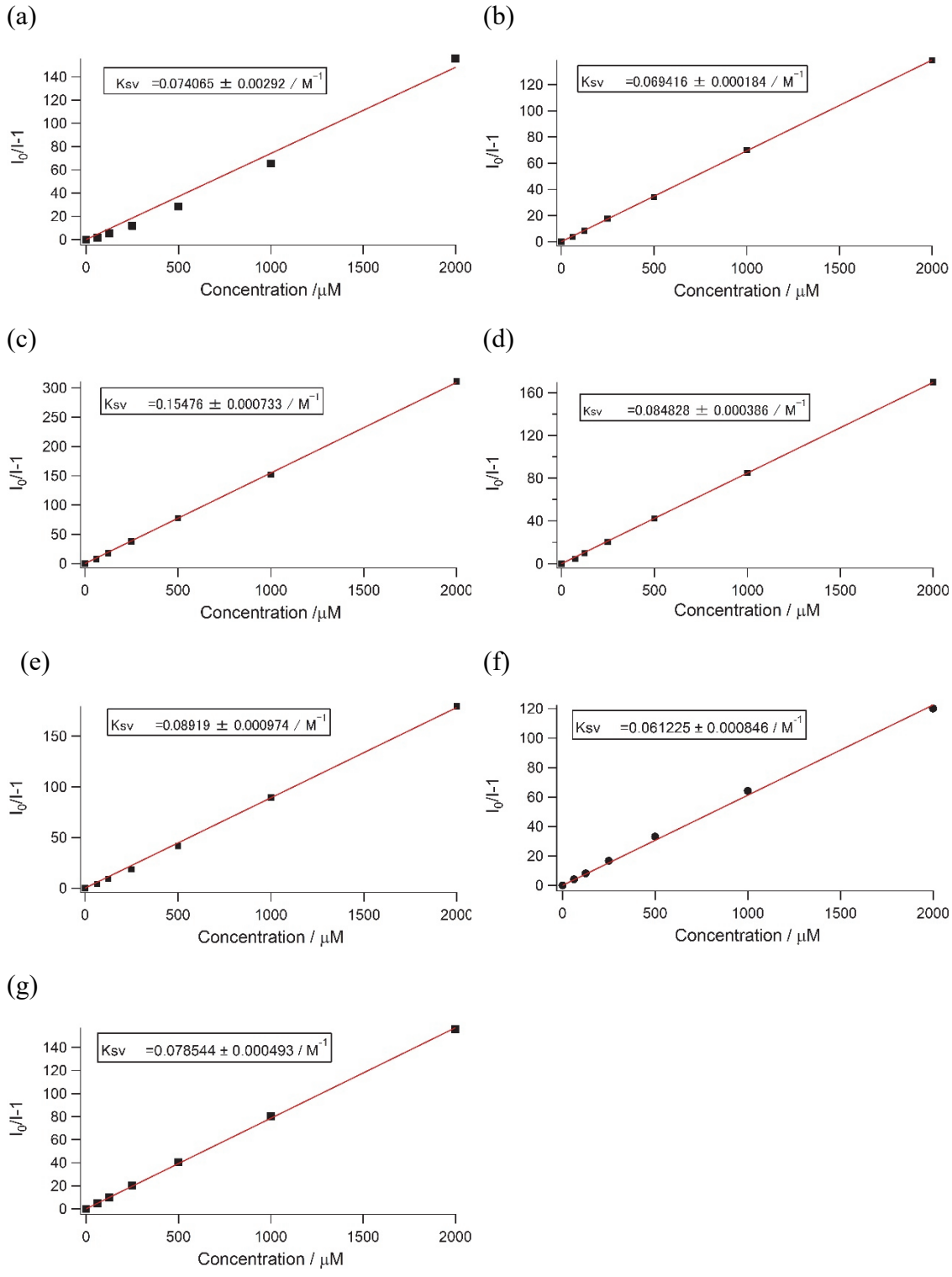

Figure S3. Stern-Volmer plots of (a) unsub. DPH, (b) NO_2 DPH, (c) NMe_2 DPH, (d) CN DPH, (e) CF_3 DPH, (f) pico DPH and (g) jul DPH dissolved with PdTPBP (20 μM) in THF. The concentrations of DPH derivatives were 0, 65, 125, 250, 500, 1000 and 2000 μM.

(a)

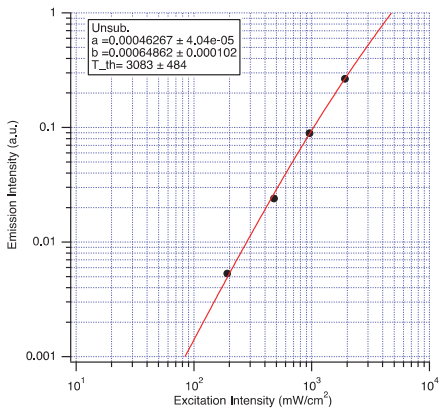
Unsub.
a =0.00046267 ± 4.04e-05
b =0.00064862 ± 0.000102
T_th= 3083 ± 484
Emission Intensity (a.u.)
Excitation Intensity (mW/cm²)

(b)

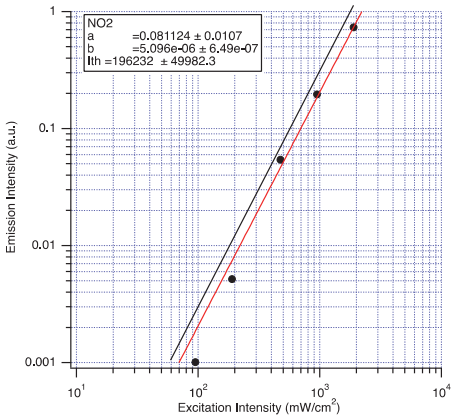
NO2
a =0.081124 ± 0.0107
b =5.096e-06 ± 6.49e-07
Ith =196232 ± 49982.3
Emission Intensity (a.u.)
Excitation Intensity (mW/cm²)

(c)

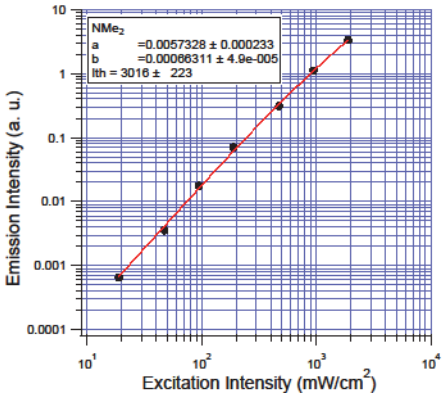
NMe2
a =0.0057328 ± 0.000233
b =0.00066311 ± 4.9e-005
Ith = 3016 ± 223
Emission Intensity (a. u.)
Excitation Intensity (mW/cm²)

(d)

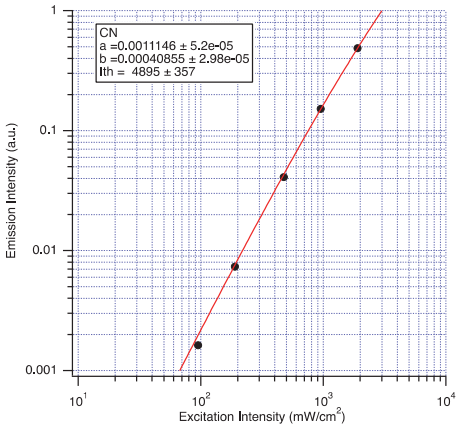
CN
a =0.0011146 ± 5.2e-05
b =0.00040855 ± 2.98e-05
Ith = 4895 ± 357
Emission Intensity (a.u.)
Excitation Intensity (mW/cm²)

(e)

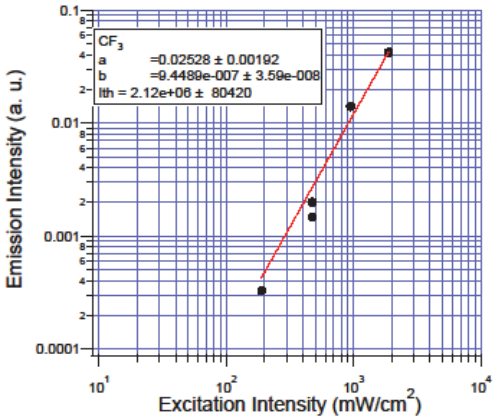
CF3
a =0.02528 ± 0.00192
b =9.4489e-007 ± 3.59e-008
Ith = 2.12e+06 ± 80420
Emission Intensity (a. u.)
Excitation Intensity (mW/cm²)

(f)

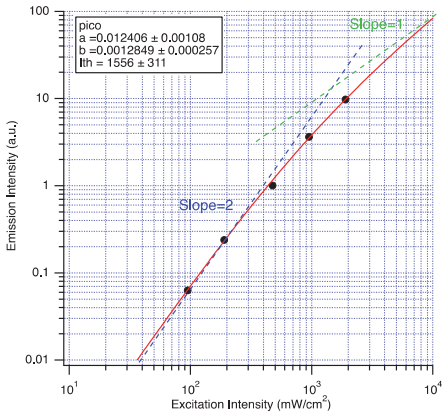
pico
a =0.012406 ± 0.00108
b =0.0012849 ± 0.000257
Ith = 1556 ± 311
Slope=1
Slope=2
Emission Intensity (a.u.)
Excitation Intensity (mW/cm²)

(g)

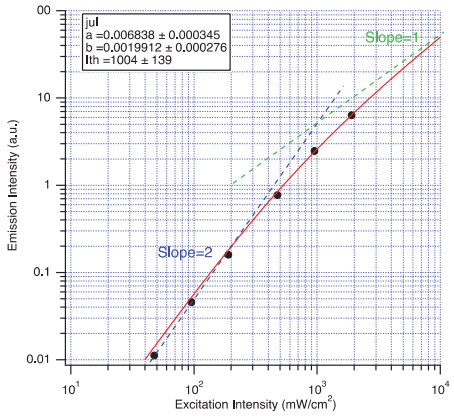

Figure S4. UC emission intensities of (a) unsub. DPH, (b) NO_2 DPH, (c) NMe_2 DPH, (d) CN DPH, (e) CF_3 DPH, (f) pico DPH and (g) jul DPH dissolved with PdTPBP (20 µM) in THF for different excitation intensities with the curve fit according to Eq. (36), Ref. 4. Reliable values for NO_2 and CF_3 could not be obtained because I_{th} is too high compared to the range of the excitation intensity employed.

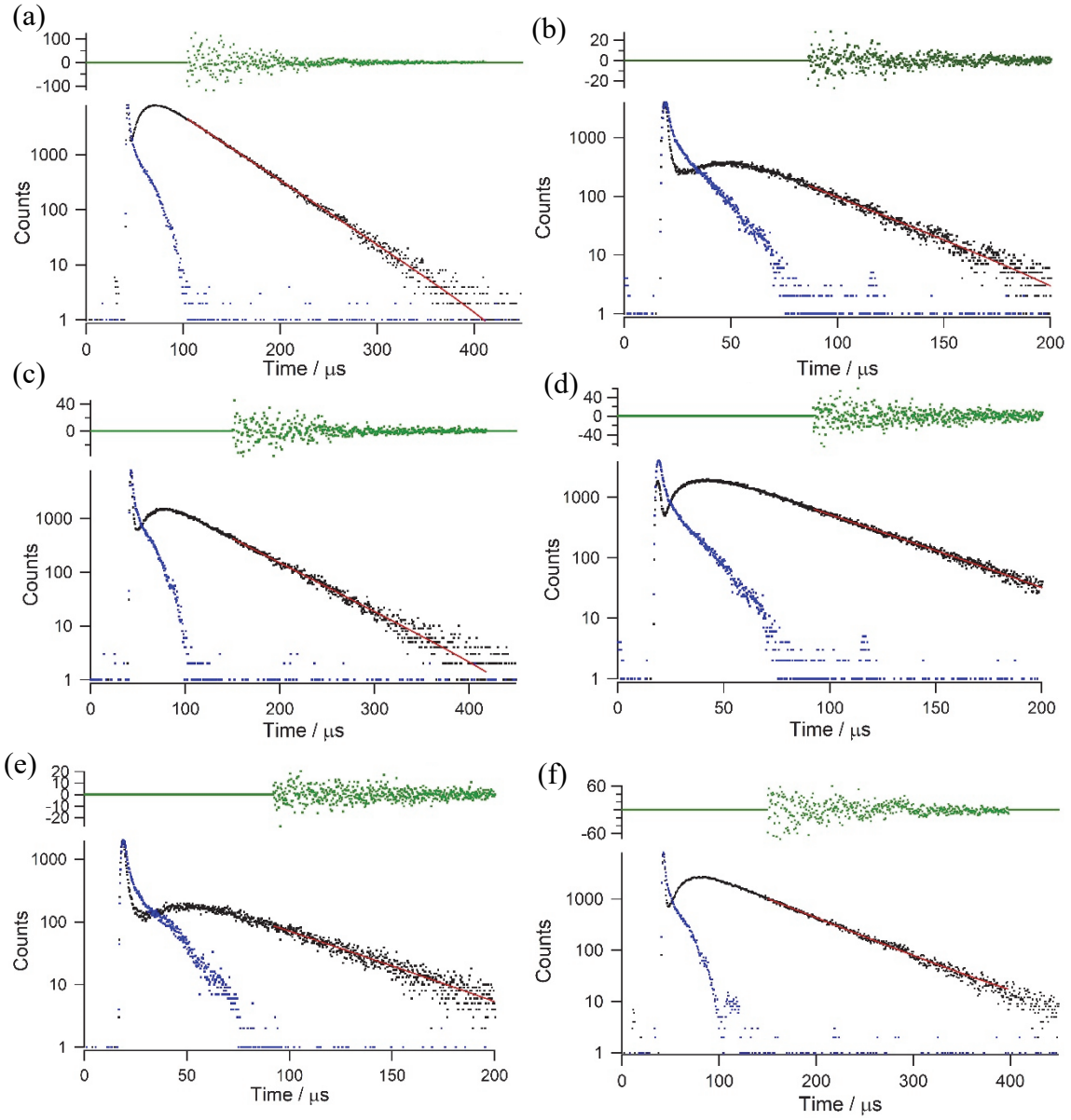

Figure S5. Time profiles of UC emission (black dots) of (a) unsub. DPH, (b) NO_2 DPH, (c) NMe_2 DPH, (d) CN DPH, (e) CF_3 DPH, (f) jul DPH mixed with PdTPBP in solution (PdTPBP 20 µM–DPHs 125 µM in THF) in N_2 atmosphere, together with their fit (red line), instrument response function (IRF, blue dots) and residuals (green dots).

References

[1] X. Peng, J. Du, J. Fan, J. Wang, Y. Wu, Ji. Zhao, S. Sun, and T. Xu, *J. Am. Chem. Soc.* **129**, 1500 (2007).

[2] T. Yanai, D. P. Tew, and N. C. Handy*, Chem. Phys. Lett.* **393**, 51 (2004).

[3] Gaussian 16, Revision C.01, M. J. Frisch, G. W. Trucks, H. B. Schlegel, G. E. Scuseria, M. A. Robb, J. R. Cheeseman, G. Scalmani, V. Barone, G. A. Petersson, H. Nakatsuji, X. Li, M. Caricato, A. V. Marenich, J. Bloino, B. G. Janesko, R. Gomperts, B. Mennucci, H. P. Hratchian, J. V. Ortiz, A. F. Izmaylov, J. L. Sonnenberg, D. Williams-Young, F. Ding, F. Lipparini, F. Egidi, J. Goings, B. Peng, A. Petrone, T. Henderson, D. Ranasinghe, V. G. Zakrzewski, J. Gao, N. Rega, G. Zheng, W. Liang, M. Hada, M. Ehara, K. Toyota, R. Fukuda, J. Hasegawa, M. Ishida, T. Nakajima, Y. Honda, O. Kitao, H. Nakai, T. Vreven, K. Throssell, J. A. Montgomery, Jr., J. E. Peralta, F. Ogliaro, M. J. Bearpark, J. J. Heyd, E. N. Brothers, K. N. Kudin, V. N. Staroverov, T. A. Keith, R. Kobayashi, J. Normand, K. Raghavachari, A. P. Rendell, J. C. Burant, S. S. Iyengar, J. Tomasi, M. Cossi, J. M. Millam, M. Klene, C. Adamo, R. Cammi, J. W. Ochterski, R. L. Martin, K. Morokuma, O. Farkas, J. B. Foresman, and D. J. Fox, Gaussian, Inc., Wallingford CT (2019).

[4] Y. Murakami and K. Kamada, *Phys. Chem. Chem. Phys.* **23**, 18268 (2021).